

# Sympathetic cooling of ${}^4\text{He}^+$ ions in a radiofrequency trap

B. Roth, U. Fröhlich, and S. Schiller

*Institut für Experimentalphysik, Heinrich-Heine-Universität Düsseldorf, 40225 Düsseldorf, Germany*

We have generated Coulomb crystals of ultracold  ${}^4\text{He}^+$  ions in a linear radiofrequency trap, by sympathetic cooling via laser-cooled  ${}^9\text{Be}^+$ . Stable crystals containing up to 150 localized  $\text{He}^+$  ions at  $\sim 20$  mK were obtained. Ensembles or single ultracold  $\text{He}^+$  ions open up interesting perspectives for performing precision tests of QED and measurements of nuclear radii. The present work also indicates the feasibility of cooling and crystallizing highly charged atomic ions using  ${}^9\text{Be}^+$  as coolant.

The two-body Coulomb system is one of the most fundamental in physics, and has been central in the development of quantum mechanics, relativistic quantum mechanics, and QED. In nuclear physics, the study of these systems can provide an alternative method for precise determination of nuclear sizes [1]. Hydrogen-like systems studied include the hydrogen atom and its isotopes, muonic hydrogen, the helium ions, muonium and positronium. More recently, heavy (high- $Z$ ) hydrogen-like ions have become available [2] and are being used e.g. for exploring strong-field QED [3], and for measuring the electron mass [4]. Among the low- $Z$  atomic systems, hydrogen has been the most extensively studied, in particular by laser spectroscopy. This has resulted, among others, in the most precise measurement of a fundamental constant, the Rydberg constant [5]. While the helium ions  ${}^3\text{He}^+$  and  ${}^4\text{He}^+$  are important systems because they are complementary to the hydrogen atom, they have been much less studied. Precision measurements of transition frequencies in  $\text{He}^+$  ions could provide (i) an independent (metrologically significant) determination of the Rydberg constant, (ii) an independent determination of the nuclear charge radii and the isotope shift, assuming QED (Lamb shift) calculations are correct, or (iii) a test of QED, using independent radius data (from scattering measurements) as input.

Precise values of the He nuclear radii can test theoretical nuclear methods and force models, which accurately describe these special nuclei ( ${}^3\text{He}$  is the only stable three-particle nucleus,  ${}^4\text{He}$  is lightest closed-shell nucleus). The possibility of QED tests with He ions is attractive because the QED corrections scale with high powers of  $Z$  (some of the theoretically unknown contributions scale as  $Z^6$ ), and thus their relative contribution to transition frequencies is larger than in hydrogen. Also, the available independent  ${}^4\text{He}^+$  radius measurements agree, in contrast to the situation in hydrogen.

On the experimental side, the hyperfine structure of  ${}^3\text{He}^+$  has been measured both in the electronic 1S ground state and the 2S excited state [6]. The Lamb shift of the 2S state in  ${}^4\text{He}^+$  has been determined from the spontaneous emission anisotropy with 170 kHz uncertainty and compared to theoretical calculations [7, 8]. The  ${}^3\text{He}/{}^4\text{He}$  squared nuclear radius difference has been determined at the 0.4% level from the isotope shift in

neutral Helium using laser spectroscopy [9].

A significant extension of these studies would be accessible via high-resolution laser spectroscopy of helium ions, which has not been performed so far. Measurements of the 1S - 2S and 2S - 3S two-photon transition frequencies (at 61 nm and 328 nm, with linewidths 167 Hz and 16 MHz, respectively) have been proposed [10, 11]. For example, a 1S - 2S measurement with reasonable experimental uncertainty  $< 30$  kHz would test the nuclear and the recently improved theoretical QED contributions at their current accuracy level [12]. A measurement of the isotope shift with a similar accuracy would improve the value of the squared nuclear charge radius difference by an order of magnitude.

One important aspect in these future precision experiments will be the availability of trapped ultracold helium ions, in order to minimize or eliminate the influence of Doppler broadening or shifts, and to allow a precise study of systematic effects. The experience with trapped ions for atomic clocks has shown the success of this approach [13].

In this work we report on the first production of an ultracold sample of  ${}^4\text{He}^+$ . While trapping of these ions is straightforward using a Paul-type trap [14], cooling is more difficult. Direct laser cooling appears impractical at present, since the generation of the required continuous-wave deep-UV 30 nm radiation is a challenging problem in itself. An alternative and flexible method is sympathetic (interaction) cooling, where "sample" particles of one species are cooled by an ensemble of directly cooled (often by laser cooling) particles of another species via their mutual interaction. This method was first demonstrated for ions in Penning traps [15, 16], and later in Paul traps [17, 18, 19]. Under strong cooling, the mixed-species ensemble forms a Coulomb crystal. In sympathetic crystallization of large ensembles a minimum mass ratio range  $m_{sc}/m_{lc}$  of 0.6 between sympathetically cooled and laser-cooled ions has so far been achieved [20]. Recent molecular dynamics simulations showed that sympathetic cooling in an ion trap down to a mass ratio of 0.3 should be possible [21, 22]. A two-ion sympathetically cooled crystal exhibited a mass ratio of 0.38 [23]. In the present work we have used the lightest atomic ion suitable for practical laser cooling,  ${}^9\text{Be}^+$ , for which the mass ratio to  ${}^4\text{He}^+$  is 0.44.

We use a linear quadrupole trap to simultaneously store  $\text{Be}^+$  and  $\text{He}^+$  ions. The trap is enclosed in a ultra-high vacuum chamber kept below  $1 \times 10^{-10}$  mbar and consists of four cylindrical electrodes, each sectioned longitudinally into three parts. The overall length of the electrodes is 10 cm, the central region being 1.6 cm long. A necessary condition for stable trapping of noninteracting ions is a Mathieu stability parameter,  $q = 2QV_{RF}/m\Omega^2r_0^2$ ,  $< 0.9$ . Here,  $Q$  and  $m$  are the charge and the mass of the trapped ions,  $V_{RF}$  and  $\Omega$  are the amplitude and the frequency of the rf driving field and  $r_0 = 4.3$  mm is the distance from the trap centerline to the electrodes. Trap operation at small  $q$  parameters is favorable since rf-heating effects are less pronounced. We operate our trap at an rf frequency of  $\Omega = 2\pi \cdot 14.2$  MHz and an rf amplitude of 380 V where the stability parameter is  $q \simeq 0.04$  (0.1) for  $\text{Be}^+$  ( $\text{He}^+$ ) ions. For such small  $q$  one can approximate the motion of ions (in absence of interactions) by that in an effective time-independent harmonic potential

$$U_{\text{trap}}(x, y, z) = \frac{m}{2}(\omega_r^2(x^2 + y^2) + \omega_z^2z^2) \quad (1)$$

The  $z$ -axis is along the trap centerline. Oscillations transverse to the  $z$ -axis occur with frequency  $\omega_r = (\omega_0^2 - \omega_z^2/2)^{1/2}$ , with  $\omega_0 = QV_{RF}/\sqrt{2}m\Omega r_0^2$  being the limiting value for a very prolate trap. The longitudinal frequency  $\omega_z = (2\kappa QV_{EC}/m)^{1/2}$  is obtained from a dc potential  $V_{EC}$  applied to the 8 end sections (endcaps) of the electrodes, where  $\kappa \approx 3 \cdot 10^{-3}/\text{mm}^2$  is a constant determined by the trap geometry.

For laser cooling of  $\text{Be}^+$  ions we produce light resonant with the  $^2S_{1/2}(F=2) \rightarrow ^2P_{3/2}$  transition at 313 nm. We employ doubly-resonant sum frequency generation (SFG) of two solid-state laser sources, a resonantly doubled Nd:YAG laser (532 nm), and a Ti:Sapphire laser at 760 nm, in a bow-tie shaped ring cavity containing an LBO crystal [24]. The Nd:YAG laser is the master laser and is frequency stabilized to a hyperfine transition of molecular iodine. By slaving the SFG cavity to the master laser and locking the Ti:Sapphire to the cavity, the sum frequency wave is also frequency stabilized. An AOM placed before the iodine stabilization setup allows to shift the UV frequency within a range of 340 MHz while maintaining absolute frequency stability. When the iodine stabilization is switched off, the continuous tuning range exceeds 16 GHz. UV output powers of up to 100 mW were obtained. Since the Doppler cooling transition is not a closed transition spontaneous emission to the metastable ground state  $^2S_{1/2}(F=1)$  is possible. This population is removed using repumping light red detuned by 1.250 GHz, produced by an electrooptic modulator. To minimize the effect of radiation pressure force on the crystal shape we usually use two counterpropagating laser beams. The  $\text{Be}^+$  fluorescence is simultaneously recorded with a photomultiplier and a CCD camera.

Our basic procedure is as follows: first, we load the trap with  $\text{He}^+$  ions by leaking He gas into the vacuum chamber at a pressure of  $10^{-8}$  mbar and ionizing it in situ by a 750 eV electron beam crossing the trap center. The loading rate is controlled by the partial pressure of neutral He gas and the electron beam intensity. After allowing for the He pressure to drop to the initial value,  $\text{Be}^+$  ions are produced by ionizing neutral atoms evaporated from a Be oven with the same electron beam. During  $\text{Be}^+$  loading the cooling and repumper lasers are continuously scanned over a 5 GHz interval below resonance. If necessary, mass-selective cleaning of the trap is applied to eject heavy impurity particles prior to crystallization. To this end, we add a static quadrupole potential  $V_{DC}$  to the trap until the  $a$  parameters ( $a = 4QV_{DC}/m\Omega^2r_0^2$ ) of the unwanted species lie outside the Mathieu stability range. Thus, stable trapping of particles exceeding the mass of the atomic coolants is prevented.

One of the well-known signs for a phase transition from the fluid ion plasma to an ordered crystal state is the appearance of a sudden drop in the detected fluorescence attributed to the reduction in the particle velocities and thus Doppler broadening. Once this occurs, the cooling laser frequency is held constant at a red detuning of approx. half the natural linewidth (60 MHz) from the  $\text{Be}^+$  resonance. Under this condition the crystals are stable, with a particle loss half time of  $\sim 3$  h.

Fig.1 shows three prolate two-component ion crystals containing  $\text{Be}^+$  and  $\text{He}^+$ . The crystals display the well-known shell structure and enclose an inner dark region originating from the incorporated sympathetically cooled particles having a lower mass-to-charge ratio than that of the atomic coolants. Their location on-axis is due to the stronger effective potential ( $\sim Q^2/m$  for a strongly prolate trap,  $\omega_r \gg \omega_z$ ) experienced by them as compared to the  $\text{Be}^+$  ions, see Eq.(1). While Fig.1 a was taken with an axially symmetric potential, in Fig.1 b,c a static quadrupole potential  $V_{DC}$  was added so as to make the region occupied by the  $\text{He}^+$  more visible. The added potential turns the spheroidal crystal into an ellipsoid, squeezing the crystal in a direction at  $45^\circ$  to the observation direction [25]. This results in a redistribution of the ions such that fewer or no  $\text{Be}^+$  ions remain in front and behind the  $\text{He}^+$  ions. The shapes of large Coulomb crystals containing a small relative amount of  $\text{He}^+$  ions agree well with the cold fluid plasma model [25, 26].

The number of crystallized particles is estimated by performing molecular dynamics (MD) simulations and varying the number of particles until the observed CCD image is reproduced. While for single-species structures one may obtain the particle number from the cold fluid model, which yields a particle density  $n_0 = \epsilon_0 V_{RF}^2/m\Omega^2r_0^4$  ( $\approx 3.1 \times 10^4/\text{mm}^3$  for  $\text{Be}^+$ ), together with measured dimensions, here the MD approach is better suited. It is applicable to multi-species structures, in addition produces detailed structural information, and

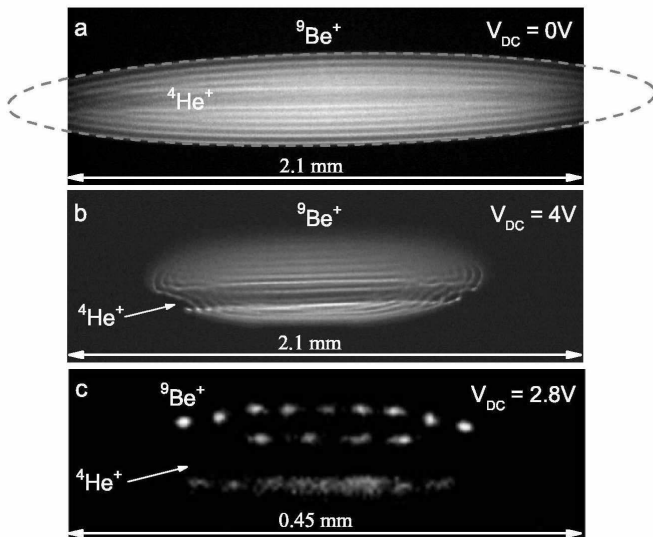


FIG. 1: CCD images of two-component Coulomb crystals (camera integration time: 2s). (a): spheroidal crystal. The ellipse is a fit to the crystal boundary with a semi-axes ratio  $R/L = 0.16$ . (b,c): ellipsoidal crystal. The inner dark cores contain approx. 150, 30, and 5 sympathetically crystallized  $\text{He}^+$  ions, respectively. The trap axis  $z$  is horizontal. For (a,c) the cooling laser beam direction is to the right, for (b) two counterpropagating beams were used. The asymmetric ion distribution for (b,c) is attributed to static stray potentials.

reduces uncertainties related to the calibration of the imaging system magnification. For example, MD simulations of the crystal in Fig.1a show that it contains approximately  $6.2 \times 10^3$   $\text{Be}^+$  ions and 150  $\text{He}^+$  ions. The radial intershell distance is obtained as  $29 \mu\text{m}$ . This value agrees well with the result calculated for infinite planar plasma crystals,  $1.48 (3/4\pi n_0)^{1/3} = 29.2 \mu\text{m}$ . According to the simulations, the  $\text{He}^+$  ions are arranged in a zig-zag configuration along the trap axis for two-thirds of the crystal, with a pitch spacing of  $\approx 40 \mu\text{m}$ . In the remaining third (left end of the crystal) the  $\text{He}^+$  ions form a linear string, as evidenced by the smaller radial extension of the inner dark core. The asymmetric distribution is caused by light pressure forces on the  $\text{Be}^+$  ions. Embedded strings were also observed in a mixed crystal of  $\text{Ca}^+$  and  $\text{Mg}^+$  ions where both ions were laser cooled [27].

An alternative way to roughly estimate the number of sympathetically cooled  $\text{He}^+$  ions is as follows. Crystallized ions of any species are in force equilibrium at their locations  $\mathbf{r}_i$ . Thus, in a region occupied by a particular species, the space charge electric field takes on the values  $Q\mathbf{E}(\mathbf{r}_i) = \nabla U_{\text{trap}}(\mathbf{r}_i)$ . Consider now a closed smooth surface that is chosen such that it closely approaches many ion loci  $\mathbf{r}_i$ . We assume this relation approximately holds on the entire surface. Applying Gauss' law, the total charge  $Q_e$  enclosed by the surface is given

by  $Q_e = \epsilon_0 V_e \Delta U_{\text{trap}}/Q$ , where  $V_e$  is the volume enclosed by the surface and a harmonic trap has been assumed,  $\Delta U_{\text{trap}}(\mathbf{r}) = \text{const}$ . The Laplacian also determines the constant charge density  $\rho = \epsilon_0 \Delta U_{\text{trap}}/Q = n_0 Q$  of an ion species within the liquid charge model. Thus, the enclosed charge is simply the "displaced charge",  $Q_e = \rho V_e$ . We now apply this to the heavier particle species surrounding a cylindrical core containing lighter ions. Taking as the surface the cylinder bounded by the innermost  $\text{Be}^+$ -shell in Fig. 1 a (radius  $r_{\text{shell}} \approx 35 \mu\text{m}$ ) and extending to the ends of the dark core (length  $\approx 2.2$  mm), the estimate for the light species number is  $N_{\text{He}} = Q_e/Q_{\text{He}} = Q_{\text{Be}} n_{0,\text{Be}} V_e / Q_{\text{He}} \approx 260$ . This is in reasonable agreement (within a factor of 2) with the MD simulations, considering that  $r_{\text{shell}}$  clearly varies over the crystal length and the approximations made.

In order to identify the sympathetically cooled and crystallized ions we have performed mass spectroscopy by mass-selective excitation of transverse (secular) motion in the trap. A plate electrode was placed between two trap rods and an ac voltage applied (1 V amplitude). A secular scan is taken by varying the excitation frequency  $\omega_{\text{ext}}/2\pi$  and recording the  $\text{Be}^+$  fluorescence with the photomultiplier. The secular excitation pumps energy into the crystal; the resulting higher  $\text{Be}^+$  ion velocities imply a line broadening. This leads to less fluorescence if the laser frequency lies near resonance, as is the case when the detuning is optimized for maximum cooling. This effect occurs for excitation of any species: since the species are strongly coupled by Coulomb interaction, heating of one species will lead to energy transfer to the others.

Fig.2 shows images for a large two-component ion crystal before (a) and after (c) secular scans. Initially, the secular scan shows the presence of both  $\text{Be}^+$  (resonance at 283 kHz) and  $\text{He}^+$  (685 kHz). The former value is close to the calculated value of 271 kHz. Regarding the  $\text{He}^+$  resonance, we notice both an increase in fluorescence before resonance, and a substantial shift of the resonance peak from the theoretical value (613 kHz). We attribute this spread and shift to a modification of the secular frequency  $\omega_r$ , which is a single-particle property, by the  $z$ -dependence of the  $\text{Be}^+$  ion distribution. The permanent increase of the fluorescence intensity level before reaching the sharp  $\text{He}^+$  secular excitation peak is due to removal of  $\text{He}^+$  ions from certain regions of the crystal by the high excitation amplitude.

After a few secular excitation cycles the  $\text{He}^+$  ions were nearly completely removed from the trap, Fig. 2 c, leaving behind a nearly pure  $\text{Be}^+$  ion crystal, as evidenced by the absence of secular resonance in Fig. 2 d. The small number of impurities remaining in the left end of the crystal did not lead to a fluorescence signal. Note that the visible crystal size has decreased substantially because of  $\text{Be}^+$  ion loss. Nevertheless, the absolute fluorescence intensity of the final  $\text{Be}^+$  crystal is essentially equal to the level at the end of the first secular scan. This may

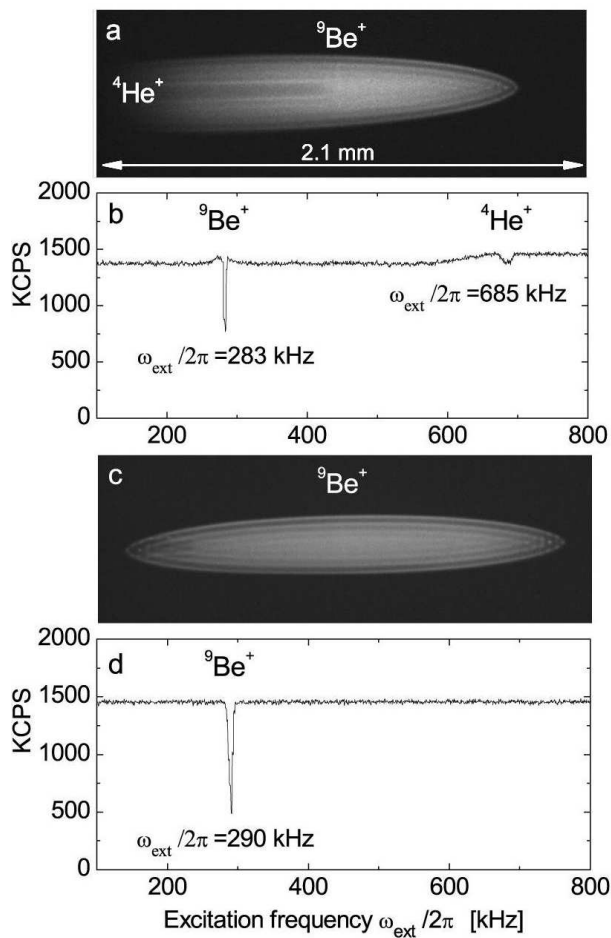


FIG. 2: (a): Prolate two-component Coulomb crystal (cooling laser beam direction to the right). (b): corresponding  $\text{Be}^+$  fluorescence signal as a function of secular excitation frequency  $\omega_{\text{ext}}/2\pi$ . (c): ion crystal after removal of  $\text{He}^+$  through repeated secular excitation. (d): corresponding secular excitation spectrum. Time between Fig. (a,b) and (c,d): 5 min. Frequency scans are toward increasing frequency.

be explained by a lower ion temperature or reduced micromotion. Moreover, a shift of the crystal with respect to the trap occurred in the direction of the propagation of the laser beam. We attribute this to stronger light pressure forces experienced by the  $\text{Be}^+$  ions, which is consistent with the increased fluorescence level per ion. A central question concerning sympathetically cooled ions is their translational temperature; several observations can shed light on the answer. A direct measurement on  $^{24}\text{Mg}^+$  embedded in a laser-cooled  $^{40}\text{Ca}^+$  crystal yielded an upper limit of 45 mK, deduced from the  $^{24}\text{Mg}^+$  laser excitation linewidth [20]. In a two-ion crystal sympathetic cooling to the Doppler-limit ( $<1$  mK) has been shown [23]. MD simulations for small particle numbers have shown that sympathetic ions caged by laser-cooled ions are essentially in thermal equilibrium with the latter at the Doppler temperature [22]. Thus, an estimate

of the sympathetic temperature may be obtained from the temperature of the laser-cooled ions. We deduce a direct upper limit for the translational temperature of the  $\text{Be}^+$  ions from the spectral line shape of their fluorescence as the cooling laser is tuned towards resonance and the ion ensemble crystallizes. Since the temperature of the particles changes during the frequency scan, we fit an appropriate Voigt profile to each point of the recorded fluorescence curve to determine the  $\text{Be}^+$  temperature. For small crystals ( $<1000$  particles), we find an upper limit for the temperature at the end of the scan of 42 mK. An indirect upper limit is obtained by comparing the size of the ion spots with MD simulations; here we find a tighter limit of  $<20$  mK for the  $\text{Be}^+$  temperature. We therefore deduce, assuming thermal equilibrium, that the  $\text{He}^+$  temperature is  $<20$  mK.

In summary, we have sympathetically cooled and crystallized  $\text{He}^+$  ions using laser-cooled  $\text{Be}^+$  ions in a linear Paul trap. Large Coulomb crystals of  $\sim 6.2 \times 10^3$   $\text{Be}^+$  ions contained about 150  $\text{He}^+$  ions, arranged in a zig-zag structure centered on the trap axis. The mass ratio of 0.44 between sympathetically cooled and laser-cooled ions is the lowest achieved so far for large ion ensembles in a Paul trap. We estimate the temperature of the crystallized  $\text{He}^+$  ions at below 20 mK.

Translationally cold and immobilized  $\text{He}^+$  ions are a promising system for high precision spectroscopy and might lead to more precise atomic and nuclear constants. The weak  $1S - 2S$  transition in  $\text{He}^+$  could be detected with high signal to noise ratio using a single adjacent  $\text{Be}^+$  ion as a "quantum sensor", rather than by direct detection of its fluorescence [28]. Significant progress in this direction has been achieved [23, 29]. Moreover, sympathetically cooled  $\text{He}^+$  opens up perspectives for studies of cold collisions and cold chemistry, e.g. generation of  $^3\text{HeH}^+$  molecules, whose hyperfine structure is of interest in fundamental physics [30].

The  $^4\text{He}^+ / ^9\text{Be}^+$  cooling and crystallization results also have implications for the possibility of achieving this with highly charged atomic ions (HCAI). Favorably, the  $q$  parameters are similar and the effective potential, Eq. (1), is steeper for the HCAIs than for the  $^9\text{Be}^+$ . Under appropriate conditions, the laser-cooled  $^9\text{Be}^+$  ions are expected to cage the HCAIs, leading to efficient cooling, as demonstrated with  $^4\text{He}^+$ .

We thank the Deutsche Forschungsgemeinschaft (DFG) and the EU network HPRN-CT-2002-00290 for support. We are grateful to D. Leibfried for helpful suggestions, H. Wenz for the MD simulations, and S. Karshenboim for discussions.

Note added in proof: We have also produced two-species Coulomb crystals containing  $^3\text{He}^+$ .

- 
- [1] See, e.g., *Precision physics of simple atomic systems*, S.G. Karshenboim et al., eds. (Springer, 2001); M.I. Eides et al., *Phys. Rep.* **342**, 63 (2001).
- [2] J.D. Gillaspay, *J. of Phys. B* **34**, R93 (2001).
- [3] See e.g., V.M. Shabaev et al., *Phys. Rev. Lett.* **86**, 3959 (2001) and references therein.
- [4] J. Verdu et al., *Phys. Rev. Lett.* **92**, 093002 (2004).
- [5] B. de Beauvoir et al., *Eur. Phys. J. D* **12**, 61 (2000).
- [6] H.A. Schuessler et al., *Phys. Rev.* **187**, 5 (1969); M.H. Prior, E.C. Wang, *Phys. Rev. A* **16**, 6 (1977); for the theory, see S.G. Karshenboim, V.G. Ivanov, *Eur. Phys. J. D* **19**, 13 (2002).
- [7] A. van Wijngaarden et al., *Phys. Rev. A* **63**, 012505 (2000).
- [8] U.D. Jentschura, G.W.F. Drake, *Can. J. Phys.* **82**, 103 (2004).
- [9] D. Shiner et al., *Phys. Rev. Lett.* **74**, 3553 (1995).
- [10] J.L. Flowers et al., NPL report CBTLM **11** (2001); T.W. Hänsch, priv. communication.
- [11] S.A. Burrows et al., in *Laser Spectroscopy* **14**, R. Blatt et al., eds. (World Scientific, 1999).
- [12] QED uncertainty without nuclear radius effect  $\sim 6 \times 10^4$  Hz, nuclear radius effect uncertainty  $\sim 7 \times 10^4$  Hz [1, 8], uncertainty due to Rydberg constant  $\sim 8 \times 10^4$  Hz.
- For the 2S - 3S transition, the situation is somewhat less favorable due to a larger relative contribution of the  $R_\infty$  uncertainty and the larger transition linewidth.
- [13] See, e.g., Proc. of the 6th Symp. on Freq. Standards and Metrology, P. Gill, ed. (World Scientific, 2002).
- [14] F.G. Major, H.G. Dehmelt, *Phys. Rev.* **170**, 91 (1968).
- [15] R. Drullinger et al., *Appl. Phys.* **22**, 365 (1980).
- [16] D. Larson et al., *Phys. Rev. Lett.* **57**, 70 (1986).
- [17] M. Raizen et al., *Phys. Rev. A* **45**, 6493 (1992).
- [18] I. Waki et al., *Phys. Rev. Lett.* **68**, 2007 (1992).
- [19] P. Rowe et al., *Phys. Rev. Lett.* **82**, 2071 (1999).
- [20] L. Hornekær, Ph.D. thesis, Aarhus Univ. (2000).
- [21] T. Harmon et al., *Phys. Review A* **67**, 013415(8) (2003).
- [22] S. Schiller, C. Lämmerzahl, *Phys. Rev. A* **68**, 053406 (2003).
- [23] M.D. Barrett et al., *Physical Review A* **68**, 042302 (2003).
- [24] H. Schnitzler et al., *Appl. Optics* **41**, 7000 (2002).
- [25] U. Fröhlich et al., subm. to *Phys. Rev. A*.
- [26] L. Turner, *Phys. Fluids* **30**, 10 (1987).
- [27] L. Hornekær, et al., *Phys. Rev. Lett.* **86**, 1994 (2001).
- [28] D.J. Wineland et al., in [13], pp. 361-368.
- [29] B. B. Blinov et al., *Physical Review A* **65**, 040304(R) (2002).
- [30] S.G. Karshenboim, priv. communication.